

Prototyping of 3D sheet metal parts using electro hydraulic forming

J. Varis*, H. Martikka**

*Lappeenranta University of Technology, P.O.Box 20, FIN-53851 Lappeenranta, Finland; E-mail: juha.varis@lut.fi

**Lappeenranta University of Technology, P.O.Box 20, FIN-53851 Lappeenranta, Finland; E-mail: heikki.martikka@lut.fi

1. Introduction

Sheet metal forming is a widely used production method. The most popular forming method is deep drawing, which requires an accurate, robust punch and die, as well as a press with precisely controlled axes.

The high demands placed on tool technology require a high capital investment, even if numerical controlled (NC) machines have reduced production time in recent years, as have electrical discharge machines (EDM) and electrical discharge wire cutting (EDWC) machines. In the same period of time, the accuracy of tools has increased. In addition to the above-mentioned technologies, 3D CAD-programs connected directly to NC-machines have led to a reduction in the time needed for tool production.

High velocity sheet metal forming methods, such as electromagnetic forming and electro hydraulic forming (EHF), are based on high voltage electrical energy, and aroused considerable interest in the 1950's and 1960's in the USA, Japan and Russia (the former Soviet Union). In more recent decades, interest in EHF has remained at a low level. A number of commercial devices are marketed in the USA and Russia. Machines of various type and size that are available in Russia are shown in Table 1 [1]. Basics of EHF are presented in the books like by Winkler [2] and Lange [3]. Basic theory is presented in the books of Hoffman & Sachs [4], Johnson and Mellor [5] Lippman [6]. One review of EHF technology is by Klaas & al [7]. A promising tool is to use virtual model simulation using FEM programs like LS-DYNA [8].

Table 1

Machines for electrohydraulic forming on the Russian market [1]

	Udar-1	Udar-11	T1231	T123
Maximum energy of impulse, kJ	12.5	150	128	20
Maximum supply voltage, kV	10	50	40	-
Maximum dimensions for a plane piece, mm	2500x1200	2000x2000	1200x1200	650x650

Trends towards rapidly growing volumes of small series production are expected to increase the interest of high velocity forming technologies such as EHF [9]. More efficient technologies for cheaper, rapidly formed sheet metal parts are required to be available, which will be used in the manufacture of complete products. EHF is a method suitable for small series production of sheet metal and tubular parts with complex geometries. This paper presents the principle of EHF and its remarkable advantages based on simple and even low cost tool technology. Also the possibilities and experience of EHF process simulation are presented and verified for mathematical calculation.

This work is motivated by some more important trends in manufacturing technologies; sheet metal material technology has been developed recently and the properties of materials are more suitable for deformation processing. Multipurpose computer controlled machines have been developed for tool manufacturing and for process controlling. The third trend is the development of computer simulation. These trends have aroused further interest in more utilization of also EHF. One application of EHF has been presented in this paper. The application is a design-product, which has been scheduled in Fig. 6, a.

2. Materials and methods

2.1. Materials used

Material used in these tests was structural steel S235, which has initial yield strength $R_{p0.2} = 235$ MPa,

tensile strength $R_m = 360$ -510 MPa and ultimate tensile strain $A_5 = 24\%$ [10].

One useful material model for describing a plastic work hardening material is

$$\sigma = R_{p0.2} + K\varepsilon^n \quad (1)$$

where K is a work hardening coefficient; ε is a relative strain.

The model of LS-DYNA was Material Model 24 Piecewise Linear Isotropic Plasticity [8]. The von Mises yield condition can be expressed using deviatoric stress component s_{ij} , and pressure p , as

$$\varphi = J_2 - \frac{1}{3}\sigma_y^2, \quad J_2 = \frac{1}{3}s_{ij}s_{ij}, \quad s_{ij} = \sigma_{ij} - p\delta_{ij} \quad (2)$$

The yield stress σ_y is a function of effective plastic strain, ε_{eff}^p , and plastic hardening modulus, E_p . Now a linear hardening function f is used and strain rate function is set to $\beta=1$.

$$\sigma = \beta \left[R_{p0.2} + f(\varepsilon_{eff}^p) \right] \rightarrow \sigma = R_{p0.2} + E_p \varepsilon_{eff}^p$$

$$\varepsilon_{eff}^p = \int_0^t d\varepsilon_{eff}^p, \quad d\varepsilon_{eff}^p = \sqrt{\frac{2}{3} \varepsilon_{ij}^p \varepsilon_{ij}^p}, \quad E_p = \frac{EE_t}{E - E_t} \quad (3)$$

Input data was yield strength $R_{p0.2} = 235$ MPa,

Young's modulus $E = 210000$ MPa, tangent modulus $E_t = 500$ MPa and necking strain $n = 0.2$. Thus $E_p \approx 500$. Since the models describe the same material behaviour they can be equated at two points. One point is the yield point and the other is at strain $\varepsilon = 1$ giving $K = E_t$. The deformation processing was simulated using LS-DYNA program [8]. The analysis capabilities of the program include non-linear dynamic behaviour of 3D bodies with material models and the capability for using non-linear geometrical descriptions.

2.2. Electrohydraulic forming

Electrohydraulic forming (EHF) is related to the explosive forming method; the explosive additive being replaced by an electric discharge. Electrohydraulic forming is based on rapid movement and rapidly increasing pressure of water inside a chamber (Fig. 1). Water is thus used like the punch in a deep drawing process [1, 11-13].

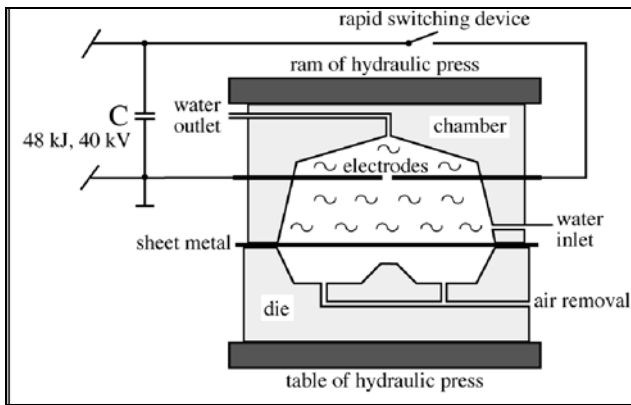


Fig. 1 Main components of electrohydraulic forming machine

The energy needed for the forming process is stored in a set of charged capacitors. The rapid switching device is closed, leading to a rapid discharge between the electrodes inside a chamber filled with water. A pressure wave is thus produced, and water is forced against the sheet to be formed, based on the design of the chamber. Depending on the material and shapes to be formed, one or several discharges are needed. The total number of discharges is also dependent on the energy used in the forming stages [14, 15].

The machine at VTT (Technical Research centre of Finland) has the following technical characteristics: maximum capacitance $60 \mu\text{F}$ ($10 \times 6 \mu\text{F}$), maximum charging voltage 40 kV , maximum impulse energy 48 kJ and impulse frequency 0.2 Hz . A set of capacitors is charged using a fully controlled three-phase six-pulse rectifier. The maximum charge can be attained every five seconds. A maximum current up to 200 kA can be achieved, and the maximum input power required is 25 kW . The machine is equipped with an automated control system, which makes it possible to set in advance the number of discharges. The mean time between discharges is around five seconds. No noticeable increase in temperature on the surface of the formed sheet is observed [14].

The forming process itself is very fast. Typically an impulse lasts no more than $200 \mu\text{s}$ and the forming

speed has been approximated to 300 m/s . A high forming speed improves the plasticity properties of the material being formed compared with traditional slower forming techniques. High forming speed also results in minimal spring-back of formed material [14].

The main advantages of electrohydraulic forming are [11]:

- minimal spring back of formed sheets because of the extremely fast forming process – the tolerance level of IT9 can normally be achieved;
- it is an extremely rapid forming process, which increases formability without the need for heat-treatment, as is the case with ordinary forming processes;
- different manufacturing processes can be combined, such as forming, punching, cropping and flanging;
- the method is well suited to small series production, since it is based on economical tool technology, which also leads to fast prototyping;
- for small batches of products with complex 3D final forms the EHF method is a cost effective method for manufacturing complex forms since only one and inexpensive die is needed and the other is replaced by hydraulic pulses as punches, contact friction is small resulting in minimal surface damage;
- modular and openable tools can be used;
- it is suited to a wide range of materials;
- EHF can be installed in a conventional hydraulic press that has sufficient free space on the table.

EHF technology shows the greatest potential for forming pieces with a low depth and a complex shape (Fig. 6). In many applications involving mild steel, plate thicknesses of three millimetres or less are involved.

2.2.1. Tool technology

The largest difference between electrohydraulic forming and so-called traditional forming processes is the tool technology. With EHF, a tool is only required on the die side. The potential of EHF is mainly based on a simple, and in many cases, economical tool technology. There is great potential for reducing tool costs. For small series production, tools can be made from common materials such as wood, plastic or even concrete. Tool steel is widely used, as well as aluminium, for small and medium sized series production [11, 14].

The chamber is made of cast steel, which also functions as the sheet holder. Three different sizes of chamber are used in the laboratory of VTT. The internal dimensions of the square-shaped chamber are $450 \times 450 \text{ mm}$. The size of the square chamber is based on the maximum volume of one pair of electrodes. Further pairs of electrodes can also be used. Two sizes of round-shaped chamber are stocked for rotating pieces, with internal diameters of 100 and 200 mm . Small holes are drilled in the base of the die to ensure the removal of air during forming. Otherwise air between a formed sheet and a die will result in imperfections in formed parts. The use of a vacuum makes the removal of air more effective.

Forming and cutting can be combined with the EHF process. Formed pieces can be cut from the blank by using a sharply-machined tool edge. Holes and gaps are produced in formed pieces in the same manner. The die is

located on a table in the hydraulic press. The chamber is opened and closed by hydraulic cylinders with a maximum force of 1.2 MN. The chamber is filled by using a continuous filling system powered by air pressure [11].

2.2.2. EHF is based on sheet drawing mechanics

The principle of a deformation process is shown in Fig. 2. These ideas are applicable also at many locations of the EHF. This rationale can be used in initial conceptual designing.

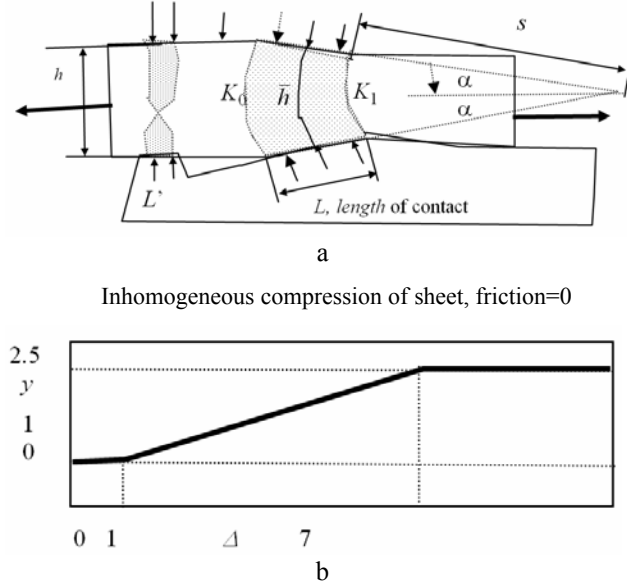


Fig. 2 Principles in a deformation process: a - geometry
b - y vs Δ schematically

In deformation processes reduction r is important. In the case of Fig. 3 it is defined as the relative change of the input arc to the output arc

$$r = 1 - \frac{K_1}{K_0} = 1 - \frac{s\alpha}{(s+L)\alpha}, \quad \frac{s}{L} = \frac{1}{r} - 1 \quad (4)$$

Another basic feature is the degree of homogeneity of the deformation defined as the ratio of mean deforming thickness to the contact length

$$\Delta = \frac{\bar{h}}{L} = \frac{1}{L} \left(s + \frac{1}{2}L \right) 2\alpha = \alpha \left(\frac{2}{r} - 1 \right) \quad (5)$$

A plane strain deformation process, like indentation, causes an inhomogeneous compression. In the case of no friction it depends on a parameter Δ

$$\left. \begin{aligned} y &= \frac{p}{2\tau_y} = 1 + 0.25(\Delta - 1) \\ \text{for } \Delta \leq 1, y &= 1; \text{ for } \Delta > 7, y \approx 2.5 \end{aligned} \right\} \quad (6)$$

here τ_y is yield strength in shear and p is pressure. In EHF sheet forming processes the y ratio can be close to 1 in thin parts and close to 2.5 in thick parts.

3. Simple analytical models

First some basic analytical models and then LS-DYNA [8] are applied to the case study; a design-product (Fig. 6, a).

3.1. Sheet flange deformation of EHF sheets

The sheet flange deformation is shown in Fig. 3. following Johnson and Mellor [5] and Hoffman and Sachs [4].

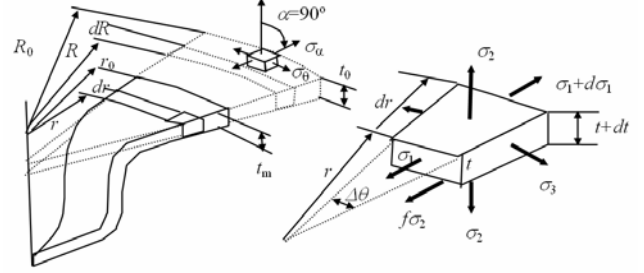


Fig. 3 Sheet flange deformation

The equilibrium of forces in the meridian direction derived by Hoffman and Sachs [4] can be used to calculate stresses by setting the meridian angle α to 90° . It is assumed that only the lower side has friction coefficient μ and the other side has smaller one due to the retainer ring

$$\begin{aligned} \frac{d(\sigma_a t r)}{dr} - \sigma_\theta t + \frac{\mu p r}{\sin \alpha} &= 0 \rightarrow \\ \rightarrow \frac{d(\sigma_1 t)}{dr} + \frac{t}{r}(\sigma_1 - \sigma_3) - \mu \sigma_2 &= 0 \end{aligned} \quad (7)$$

The principal stresses are now $\sigma_1 \rightarrow \sigma > 0$, $\sigma_2 \rightarrow 0$, $\sigma_3 < 0$. The yield criterion is now used in a compromise form between the Tresca and von Mises criteria of yielding [4]

$$\sigma_1 - \sigma_3 = m\sigma, \quad m = 1.1 \quad (8)$$

The equilibrium equation becomes

$$\frac{d(\sigma t)}{dr} + \frac{t}{r}(\sigma_1 - \sigma_3) - \mu 0 = 0 \rightarrow d\sigma + \sigma \frac{dt}{t} + \frac{dr}{r} m\sigma = 0 \quad (9)$$

Now assuming that strain rate is constant and that the change of thickness in the flange is small, $\varepsilon_t = dt/t \approx 0$, Eq. (10) predicts how the flange stress changes with radius

$$d\sigma = -\frac{dr}{r} m\sigma \quad (10)$$

Constancy of volume condition can be applied to the flange as follows

$$V = V_0, \quad \pi(r_0^2 - r^2)t_m = \pi(R_0^2 - R^2)t_0 \quad (11)$$

From which now the hoop strain may be calculated

$$\left. \begin{aligned} \left(\frac{R}{r}\right)^2 \left(\frac{t_0}{t_m}\right) - 1 &= \left(R_0^2 \frac{t_0}{t_m} - r_0^2\right) \frac{1}{r^2} = \frac{C}{r^2} \\ C = const \rightarrow \varepsilon &= \ln\left(\frac{R}{r}\right) \end{aligned} \right\} \quad (12)$$

here the thicknesses are $t_0 = 0.001$ m initially and $t_m = 0.0007$

$$\begin{aligned} C &= R_0^2 \left(\frac{t_0}{t_m} - \left(\frac{r_0}{R_0}\right)^2 \right) = \\ &= 0.07^2 \left(\frac{0.001}{0.0007} - (0.9)^2 \right) = 0.003 \end{aligned} \quad (12b)$$

The strain hardening model for the steel may be written as

$$\begin{aligned} \sigma &= R_{p0.2} + K\varepsilon^n \rightarrow R_{p0.2} + K \left(\ln \frac{R}{r} \right)^n = \\ &= R_{p0.2} + K \left(\frac{1}{2} \ln \left\{ \frac{t_m}{t_0} \left(1 + \frac{C}{r^2} \right) \right\} \right)^n \end{aligned} \quad (13)$$

The strain and yield strength at the mid cup rim
 $r = r_{end} = r_1 = 0.0225$

$$\varepsilon = \frac{1}{2} \ln \left\{ \frac{t_m}{t_0} \left(1 + \frac{C}{r^2} \right) \right\} = \frac{1}{2} \ln \left\{ \frac{0.0007}{0.001} \left(1 + \frac{0.003}{0.0225^2} \right) \right\} = 0.8$$

and $\sigma = 235 + 500 \cdot 0.8^{0.2} = 712$ MPa

This may be substituted to the equation of equilibrium, Eq. (2)

$$\left. \begin{aligned} d\sigma &= -\frac{dr}{r} mR_p - mK \left(\frac{1}{2} \ln \left\{ \frac{t_m}{t_0} \left(1 + \frac{C}{r^2} \right) \right\} \right)^n \frac{dr}{r} \\ J(r) &= \int_{r_0}^r \varepsilon^n \frac{dr}{r} \end{aligned} \right\} \quad (14)$$

The stress at the flange may be calculated, denoting by J the integral

$$\sigma = -mR_p \ln\left(\frac{r}{r_0}\right) - mK \cdot J, \quad m = 1.1 \quad (15)$$

The material strength values are here $R_{p0.2} = 235$ MPa, $n = 0.2$, $K = E_p = 500$ MPa.

Numerical results give at radius $R_0 = 0.14/2 = 0.07$ m at the mould outer radius. The outer edge is set to $r_0 = 0.63$ m $= 0.9 R_0$.

At the final inner radius $r = r_{end}$ is equal to the rim of the mould at radius $r_1 = 0.0225$, then the maximum stress is $\sigma_1 = 266 + 237 = 503$ MPa. The third principal stress is $\sigma_3 = \sigma_1 - m\sigma = 503 - 1.1 \cdot 712 = -280$ MPa.

3.2. Spherical cup models

At the product there are locations, which are deformed under pressure impact to more or less spherical form. One is the middle cup 1. Other cups are deformed at

the extensions.

Balance of forces for a cup gives, Fig. 4,

$$\begin{aligned} \Sigma F_z &= 2\pi a \sigma_s t \cos \theta - \pi a^2 p = 0 \rightarrow \sigma_s = \frac{1}{2} \frac{a}{\cos \theta} \frac{p}{t} = \\ &= p \frac{b}{2t}, \quad b = \frac{a}{\cos \theta} \quad \text{or} \quad b = \frac{a^2 + h^2}{2h} \quad \text{if} \quad b^2 = a^2 + (b-h)^2 \end{aligned} \quad (16)$$

Constancy of volume gives that the initial volume of the circular plate is the same as the volume of a spherical cup

$$V_0 = V \rightarrow \pi a^2 t_0 = 2\pi b h t \quad (17)$$

Natural thickness deformation is thus according to Lippman [6]

$$\varphi_t = \ln \frac{t_0}{t} = \ln 2 \frac{b}{a} \frac{h}{a} = \ln \left(1 + \left[\frac{h}{a} \right]^2 \right), \rightarrow \frac{t}{t_0} = \frac{1}{1 + \left[\frac{h}{a} \right]^2} \quad (18)$$

The pressure needed for hydroforming is obtained using the definition of the radius of curvature for a sphere $R = R' = -b$

$$p = \frac{2t}{b} \sigma_s = 2 \frac{t}{b} Y = 4 \frac{t_0}{a} \frac{q}{(1+q^2)^2} \sigma, \quad q = \frac{h}{a} \quad (19)$$

For an ideal plastic material with $\sigma = \text{const}$ there occurs a plastic instability which means fracture when the pressure $p(q)$ reaches a maximum value by the condition

$$\frac{dp}{dq} = 0, \quad \frac{p_{max}}{Y} = \frac{3\sqrt{3}}{4} \frac{t_0}{a}, \quad q_{max} = \frac{h_{max}}{a} = \frac{1}{\sqrt{3}} \quad (20)$$

The desired outlook proportions of the cup are obtained by rough rules connecting some dimensions as $a_1 = r_1$, $b_2 = 0.3 \cdot b_1$, $a_2 = 0.5 \cdot a_1$, $h_2 = h_1$ (Table 2).

3.3. Spherical cap compressed to contact and conform to the ogival die

The mean radius of curvature of the meridian R_1 is constant. The mean radius of the parallel circle r is expressed as by Hoffmann and Sachs [4]

$$r = r_b - R_1 (1 - \cos \alpha) \quad (21)$$

And the mean radius of curvature normal to the meridian is R_2 . It can be seen from Fig. 5

$$r = R_2 \cos \alpha, \quad dr = -R_1 d\alpha \cdot \sin \alpha, \quad t = \text{const}, \quad \tan \varphi = f \quad (22)$$

Equilibrium equations for a shell of rotational symmetry, Fig. 5, are needed.

Equilibrium of forces in the direction normal to the tangent plane gives the pressure. The equilibrium of an element in Fig. 5 gives

$$\sigma_\alpha t r d\theta d\alpha + \sigma_\theta t R_1 d\alpha d\theta \cos \alpha + p r d\theta R_1 d\alpha = 0 \quad (23)$$

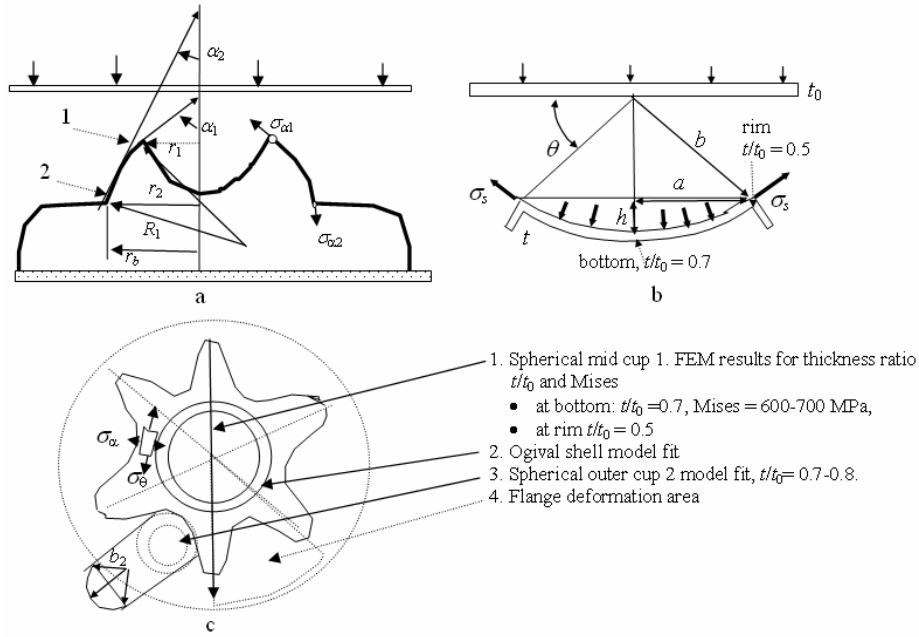


Fig. 4 Schematic models of the product (step 120): a - schematic cross section of the product; b - cup model; c - view from above

Table 2

Results of geometry changes by deformation models: a - analytical spherical cup model, no work hardening; b - LS-DYNA FEM model with work hardening. Some dimensions used the product are shown.

Initial thickness of sheet is $t_0 = t(\text{It}) = 0.001\text{m}$

Cup location IC index	Radius of the cup sphere b	Radius of circle a	Cup depth h	Allowable cup depth before instability $h_{\max} = a/3^{1/2}$	Thickness change ratio $t/t_0 = \exp(-\varphi)$	Thickness change ratio by FEM t/t_0
mid cup 1	0.031	0.022	0.009	0.013	0.86	bottom 0.7, rim 0.5
outer cup 2	0.01	0.01	0.01	0.006	0.5	0.7...0.8

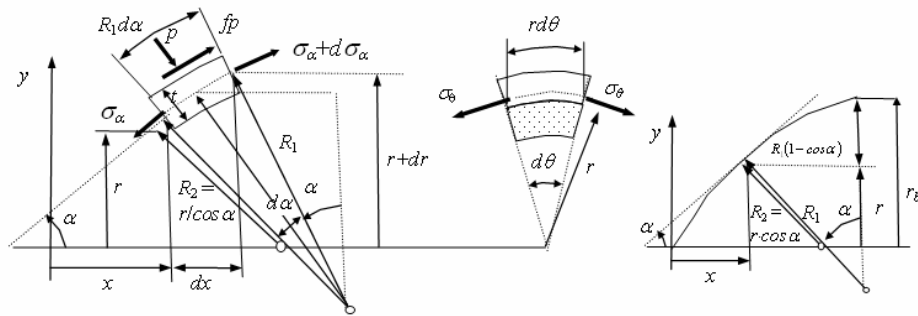


Fig. 5 Dimensions of a volume element of the shell of rotational symmetry and stresses acting on the volume element

From which one obtains

$$\frac{\sigma_\alpha}{R_1} + \frac{\sigma_\theta}{R_2} + \frac{p}{t} = 0, \rightarrow p = -t \left(\frac{\sigma_\alpha}{R_1} + \frac{\sigma_\theta \cos \alpha}{r} \right) \quad (24)$$

In this deformation process there are large compressive stresses and comparatively smaller meridian compressive stresses and yield condition is

$$\sigma_\theta < \sigma_\alpha < 0$$

whence

$$\sigma_\theta = -1.1\sigma = -m\sigma = -\sigma', \quad m = 1.1 \quad (25)$$

By substituting one obtains

$$\frac{pr}{t} = - \left(\frac{\sigma_\alpha r}{R_1} - m\sigma \cos \alpha \right) \quad (26)$$

Equilibrium of forces in the direction of the meridian tangent gives

$$(\sigma_\alpha + d\sigma_\alpha)(t+dt)(r+dr)d\theta - \sigma_\alpha t r d\theta + \sigma_\theta t R_1 d\alpha \sin \alpha d\theta + \mu p r d\theta R_1 d\alpha = 0 \quad (27)$$

From which one obtains

$$\frac{d(\sigma_\alpha t r)}{dr} - \sigma_\theta t + \frac{\mu p r}{\sin \alpha} = 0 \quad (28)$$

Equilibrium of the force components in longitudinal direction gives

$$\begin{aligned} & (\sigma_\alpha + d\sigma_\alpha)(t+dt)(r+dr)\cos(\alpha+d\alpha)d\theta - \\ & (\sigma_\alpha)(t)(r)\cos(\alpha)d\theta + pR_1d\alpha\sin\alpha d\theta + \\ & + \mu prd\theta R_1d\alpha\cos\alpha = 0 \end{aligned} \quad (29)$$

From which one obtains

$$\frac{d(\sigma_\alpha r \cos \alpha)}{dr} + pr \left(1 + \frac{\mu}{\tan \alpha}\right) = 0 \quad (30)$$

Assuming constant thickness t Eqs. (26) and (30) give

$$\frac{td(\sigma_\alpha r \cos \alpha)}{d\alpha} - prR_1 \left(\frac{\sin(\alpha + \varphi)}{\cos \varphi}\right) = 0 \quad (31)$$

Now it is assumed that pressure is increased impulsively until the sheet contacts the die and starts to bulge out of the opening of the die

$$\frac{d\left(\frac{\sigma_\alpha r}{R_1} \cos \alpha\right)}{d\alpha} - \frac{pr}{t} \left(\frac{\sin(\alpha + \varphi)}{\cos \varphi}\right) = 0 \quad (32)$$

Let us substitute here

$$\begin{aligned} X &= \frac{\sigma_\alpha r}{R_1} \\ K &= \frac{\sin(\alpha + \varphi)}{\cos \varphi} = \sin \alpha + \mu \cos \alpha = \\ &= H \sin(\alpha + \varphi) \rightarrow H = \frac{1}{\cos \varphi} \end{aligned} \quad (33)$$

And obtains

$$\frac{d(X \cos \alpha)}{d\alpha} + (X - m\sigma \cos \alpha)K = 0 \quad (34)$$

By substituting the pressure and yield condition one obtains.

$$\frac{dX}{d\alpha} + X\mu = Km\sigma, \quad \sigma' = m\sigma \quad (35)$$

The solution of Eq. (28) is the sum of two terms

$$\begin{aligned} X &= X_1 + X_2 \\ \frac{dX_1}{d\alpha} + X_1\mu &= 0, \quad \frac{dX_2}{d\alpha} + X_2\mu = \sigma' H \sin(\alpha + \varphi) \rightarrow \\ X_1 &= CY' e^{-\mu\alpha}, \quad X_2 = \sigma' [A \sin(\alpha + \varphi) + B \cos(\alpha + \varphi)] \end{aligned} \quad (36)$$

Substituting the latter trial solutions gives

$$\begin{aligned} & \sigma A \cos(\alpha + \varphi) - \sigma B \sin(\alpha + \varphi) + \\ & + \mu(A \sin(\alpha + \varphi) + B \cos(\alpha + \varphi)) = \sigma H \sin(\alpha + \varphi) \end{aligned} \quad (37)$$

From which one obtains

$$\begin{aligned} A + \mu B &= 0, \quad -B + \mu A = H \rightarrow \frac{1}{\cos \varphi} \rightarrow A = \sin \varphi, \\ B &= -\cos \varphi \end{aligned} \quad (38)$$

The solution becomes

$$\begin{aligned} X &= \sigma' [C e^{-\mu\alpha} + A \sin(\alpha + \varphi) + B \cos(\alpha + \varphi)] \\ X &= \sigma' [C e^{-\mu\alpha} + \sin \varphi \sin(\alpha + \varphi) - \cos \varphi \cos(\alpha + \varphi)] \\ X &= \sigma' [C e^{-\mu\alpha} - \cos(\alpha + 2\varphi)] = \frac{\sigma_\alpha r}{R_1} = X(\alpha) \end{aligned} \quad (39)$$

Table 3

Results as stresses and pressures of the sheet made to deform into an ogival form.
The material is S235 (IM=1)

Location of the shell Fig. 4, a	Meridional angle α	Radius of parallel circle R , m	Circumferential stress $\sigma_\theta = -m\sigma$	Meridional stress σ_α , MPa	Pressure at die p , MPa
1 (rim)	45°	0.022	-640	$\sigma = 580$	6
2 (ogival root)	17.6°	0.031	-640	150	16

At the process several boundary condition alternatives may be realized. At the upper location on the rim of the mid cup at $\alpha_1 = 45^\circ$, it is assumed that the meridional stress is about the yield strength or more at 0.2 strain assuming no description of fracture in the model

$$\begin{aligned} X_1 &= X(\alpha_1) = \sigma' [C e^{-\mu\alpha_1} - \cos(\alpha_1 + 2\varphi)] = \frac{\sigma_{\alpha_1} r_1}{R_1} \\ \sigma_{\alpha_1} &= \frac{R_1}{r(\alpha_1)} X(\alpha_1), \quad C = \left(\frac{X_1}{\sigma'} + \cos(\alpha_1 + 2\varphi)\right) e^{\mu\alpha_1} \\ X(\alpha) &= \sigma' \left[\left(\frac{X_1}{\sigma'} + \cos(\alpha_1 + 2\varphi)\right) e^{-\mu(\alpha - \alpha_1)} - \right. \\ & \left. - \cos(\alpha + 2\varphi) \right] \end{aligned} \quad (40)$$

Some results are shown in Table 3. At the mid cup bottom

$$\begin{aligned} \varepsilon_1 &= \ln \frac{t_0}{t} = \ln \left(1 + \left[\frac{h}{a}\right]^2\right) = \ln \left(1 + \left[\frac{0.009}{0.0025}\right]^2\right) = 0.15 \\ \sigma &= R_{p0.2} + K \varepsilon^n = 235 + 500 \cdot 0.15^{0.2} = 580 \end{aligned}$$

4. Virtual model forming simulations

At the case study the deformation process was simulated with LS-DYNA program. The model of LS-DYNA was Material Model 24 Piecewise Linear Isotropic Plasticity, Eq. (2). This is an elastic plastic material with an arbitrary stress versus strain curve and an arbitrary strain rate dependency can be defined.

4.1 Simulation results

Some simulation results by LS-DYNA are shown in Fig. 6.

These figures are a selection of graphic output of the program. The model is used to simulate the real manufacturing step from sheet metal to a product with desired

geometry, material strength and internal stress damage state values. The mesh of Fig. 6, a shows to the user visually the ideal surface form of the planned product. The mesh size indicates a prognosis of the calculational accuracy and power needed. This information is inputted to the program model file. Calculational outputs are shown in Figs 6, b, d.

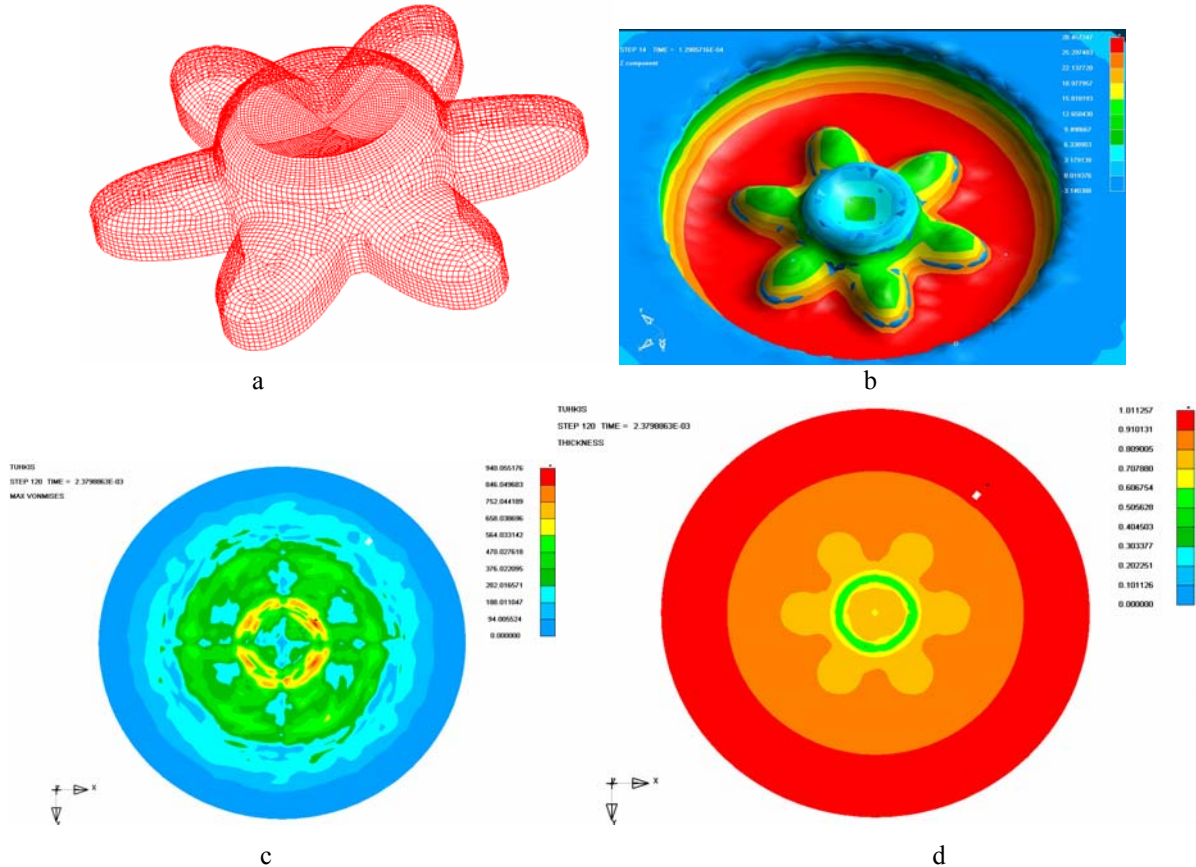


Fig. 6 Simulation results by LS-DYNA: a - the FEM mesh of the design-product; b - vertical z-depth contours; c - Von Mises stress contours at the final step (120). Max stress is 940MPa; d - thickness contours. The initial thickness is 1 mm. The mid cup bottom t/t_0 ratio is 0.7, the rim ratio is 0.5 and the outer cup model has ratio of 0.7-0.8. Rim ratio is 0.5 and the outer cup model has ratio of 0.7-0.8

The vertical z-depth contours in Fig. 6, b show visually how evenly the depths could be obtained in the calculation model. The contour variations are due to numerical error accumulation and not final product dimensional variability. Fig. 6, c shows the von Mises stress contours at the final step (120). It can be seen that the predicted max stress is rather high, 940 MPa due to the high work hardening capacity of the sheet steel and local thinning of the sheet. This information can be used to select a suitably work hardenable steel of optimal wall thickness. The thickness contours shown in Fig. 6, d indicate risk areas of the reduction. This information shows that the initial thickness of 1 mm is reduced to half at many places. The mid cup bottom t/t_0 ratio is 0.7, the rim ratio is 0.5 and the outer cup model has the ratio of 0.7-0.8. If some corrosion allowances and impact deformation resistance is required then this information is useful for redesigning the cup with higher initial thickness.

5 Conclusions

The motivation for this study was an increasing

interest in utilizing the Electro Hydraulic Forming Methods (EHF) for manufacture of advanced sheet metal products. EHF is a promising forming method for many types of formed sheet metal parts, and competes with traditional forming methods, particularly for small series production and prototyping mainly based on low tool costs. Potential users of EHF technology include companies working in the field of machining, building, ventilation, transportation, electrical, electronic, aviation and space technology.

EHF process has many design variables, what is an advantage for the designer. But the disadvantage is that their physical interdependencies are not yet clear enough for fast and easy dimensioning. But when these are mastered the full potential of this method of designing and manufacturing sheet metal products looks very promising. An efficient tool proved to be virtual engineering design FEM program LS-DYNA. It is useful for ensuring right on target designs with minimal unnecessary trials and errors.

Acknowledgements

The expert assistance of Mr. Reijo Hämäläinen in

LS-DYNA calculations and laboratory work is gratefully acknowledged.

References

1. **Varis, J. & Savinainen, T.** Electrohydraulic Forming. A work report. -VTT, Lappeenranta, Finland, 1992. -14p. (in Finnish).
2. **Winkler R.** Hoch Geschwindigkeits Bearbeitung.- Berlin: VEB Verlag Technik, 1973.
3. **Lange, K.** (editor) Handbook of Metal Forming. - McGraw-Hill Book Co, 1985.
4. **Hoffman, O. & Sachs, G.** Introduction to the Theory of Plasticity for Engineers.-New York: McGraw-Hill, 1953.
5. **Johnson, W., & Mellor, P.B.** Engineering Plasticity. - New York: Van Nostrand Reinhold Co, 1973.
6. **Lippmann.** Mechanik des Plastischen Fliessens. -Berlin: Springer-Verlag, 1981.
7. **Klaas F., Lücke U., Kaehler, K.** Developments of the Internal-High Pressure Forming Process (IHV).- Detroit: SAE International, paper 930027, 1993.
8. LS-DYNA program. 950c. Livermore Software Technology Corporation, 1997.
9. **Daehn, G.S., Altnova, M., Balanethiram, V.S., Fenton, G., Padmanabhan, M., Tamhane, A. & Winard, E.** High velocity sheet metal forming – an old technology addresses current problems.-J. of Metals (JOM), July 1995.
10. **Silvennoinen, S.** Rautaruukki Steel Products: Designers Guide, Rautaruukki, Raahе Finland, 1996, ISBN 952-5010-03-1.-272p. (in Finnish).
11. **Penttilä, R.** Electrohydraulic Forming. Research Notes no. 1808, VTT, Espoo Finland, 1997, ISBN 951-38-5083-8, ISSN 1235-0605.-35p. (in Finnish).
12. **Kujanpää, V & Varis, J.** New forming methods and applications, Ohutlevy 2/1991, p.11-12 (in Finnish).
13. **Laurila, L., Pyrhönen, J., Penttilä, R. & Kujanpää, V.** Electrohydraulic Forming. Sähkö & Tele, 1996, No5, p.23-26.
14. **Penttilä, R.** A Rapid Method for Production of Formed Sheet Metal Parts, Ohutlevy 1/1996, p.35 (in Finnish).
15. **Lohtander, M. & Varis, J.** Measurement of Active Pressure and Pressure Distribution in Electrohydraulic Forming, Lappeenranta University of Technology, Lappeenranta Finland, 2002, ISBN 951-764-654-2.-39p. (in Finnish).

J. Varis, H. Martikka

ELEKTRINIS – HIDRAULINIS 3D DETALIŲ PROTOTIPŲ FORMAVIMAS IŠ METALO LAKŠTŲ

Re z i u m ė

Elektrinis – hidraulinis formavimas (EHF) yra spartus formavimo metodas, tinkamas mažų serijų 3D detalėms gaminti. Didžiausi EHF metodo pranašumai – nebrangi technologinė įranga, didelės galimybės formuoti medžiagą, minimali įrenginio tuščioji veika. EHF metodas teikia naujų galimybių gaminti šiuolaikinius mechaninius komponentus iš metalo lakštų. Tuo siekiama padaryti perversmą detalių gamybos technologijoje. Tam tikslui reika-

lingi nauji konstravimo ir procesų imitavimo bei medžiagų patikrinimo metodai. EHF technologija taikoma Suomijoje (VTT ir LUT) bendradarbiaujant ir keičiantis technologijomis su Sankt Peterburgo universitetu (Rusija).

J. Varis, H. Martikka

PROTOTYPING OF 3D SHEET METAL PARTS USING ELECTRO HYDRAULIC FORMING

S u m m a r y

Electro hydraulic Forming (EHF) is a high speed forming method suitable for small series production of 3D sheet metal parts. The particular advantages of EHF are low cost tool technology, increased material formability, and minimal spring back. EHF of sheet metal components offers new possibilities for producing advanced components for machinery applications. This article describes the EHF process and the potential of EHF as a rapid prototyping method for sheet metal part production. The motivation is to get a breakthrough of this production technology. In addition, new design, process simulation methods and verified material models are needed. EHF technology in Finland (VTT and LUT) is based on a long-standing cooperation and technology transfer programme with the University of St. Petersburg (Russia).

И. Варис, Х. Мартиikka

ЭЛЕКТРИЧЕСКОЕ И ГИДРАВЛИЧЕСКОЕ ФОРМИРОВАНИЕ 3D ПРОТОТИПОВ ДЕТАЛЕЙ ИЗ МЕТАЛЛИЧЕСКИХ ЛИСТОВ

Р е з ю м е

Электрический и гидравлический метод формирования (ЭГФ) является методом скоростного формирования для изготовления малых серий 3D деталей из металлического листа. Особое преимущество метода ЭГФ – технологическое оборудование малых затрат, большие возможности формирования материала и минимальный холостой ход оборудования. ЭГФ метод предлагает новые возможности изготовления прогрессивных металлических компонентов из листового металла. В статье описанный ЭГФ метод и его возможности скоростного производства прототипов из металлических листов. Его мотивация – добиться переворота в указанной технологии производства. Для достижения этого необходимо дополнительно иметь новые методы конструирования и имитирования процессов, а также методов проверки материала. Технология ЭГФ в Финляндии (ВТТ и ЛУТ) основана долгосрочным сотрудничеством с Ст. Петербургом и передачей технологий.

Received January 19, 2005

DOI: 10.5755/j02.mech.13049